TD-06-029

07/21/06

Test Solenoids
Expected Performance and Test Results
Part 3: PDST03-0

R. Carcagno, C. Hess, F. Lewis, D. Orris, Y. Pischalnikov, R. Rabehl,
M. Tartaglia, I. Terechkine, J. Tompkins, T. Wokas

In this note, results of testing the third (of three) test solenoid, PDST03-0, are presented. The solenoid is similar to PDST01-0, without a flux return, and wound using Oxford rectangular strand. This note follows the pattern used in [1] and [2].

Geometrical Parameters of the Coil

Di	= 61.32 mm	Coil Inner Diameter
Do	= 93.7 mm	Outer Diameter (average; +/- 0.1)
l	= 101.5 mm	Coil Length
S	= 1644.3 mm^2	Winding Cross-Section
N	= 2000	Number of turns in the coil
n	= 22	Number of Layers
R	= 31.82 Ohm	Coil resistance at room Temperature
L	= 150 mH	Coil inductance (without Iron Yoke)

Strand

To wind the coil, Oxford NbTi rectangular strand was used

Bare strand dimensions	1.015 mm x 0.60 mm
Insulated strand dimensions	1.08 mm x 0.66 mm
Bare strand cross-section	0.604 mm^2

Other important properties that distinguish this conductor from the SSC strand are:

Cu/non-Cu ratio	1.35
Number of Filaments	54
Filament Diameter	70 μm

Coil Compaction Factor

The compaction factor was calculated as for PDST01 and was slightly lower (to our surprise): k = **0.734.** It is possible that the increased width of the strand results in lower conductor density at the ends of the coil.

Specific Features

In the coil, voltage taps were made as was done in the case of PDST01, and all the taps survived fabrication and cool down of the solenoid. For this solenoid, heaters were placed above the outer layer of the winding. Four HK5591R12.9L12B heaters were used. The size of each heater was 1.5" x 1.75" and resistance 12.9 Ohm each.

Cold Test Data

Warm magnetic measurements on PDST03-0 were taken May 9, and it was cold tested at 4.22 K with the same apparatus as PDST02-0 in the stand 3 Dewar on May 10, in a single thermal cycle. Fig. 1 shows the current history from the UNIX scan system.

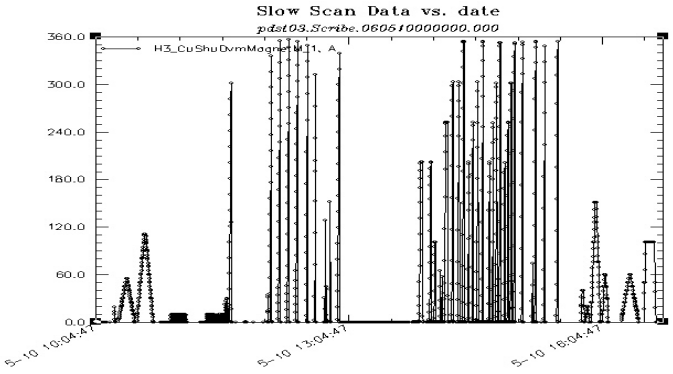

Fig. 1: Profile of PDST03 excitation current during cold testing.

Quench Current and Field Strength

Evaluation of the expected performance was made using an analytical representation of the critical surface (as measured by D. Turrioni in November, 2005) in the vicinity of the operating current:

$$Ic = 418 - 128*(B-7.0)$$

The magnetic field distribution was also evaluated analytically [3], as with PDST01-0 and PDST02-0: intersection of the strand critical surface and the solenoid load curve results in the following expected parameters at 4.2 K:

Iq	= 358.4 A	Quench Current
Bc	= 7.07 T	Central field at Quench
Bm	= 7.47 T	Maximum field in the coil
Eff	= 0.01973 T/A	Solenoid efficiency, Bc / I

No correction for the test temperature is required, and strand self-field correction makes the expected current ~ 0.5% higher, ~360.2 A. The solenoid had a very short training history, shown in Table 1: There was only one quench before maximal field was reached. The minimal quench field was ~13 % below the maximum. Ramp rate dependence shows ~6 % decline from 2 to 8 A/s.

Table 1: PDST03-0 quench currents during training and ramp rate studies

Quench #	Ramp Rate [A/s]	Quench Current [A]
1	2	320.0
2	3.8	350.3
3	2	359.4
4	2	359.6
5	2	358.1
6	4	355.4
7	8	339.5
8	23.9	250.4
9	3.8	354.6

Note that the power supply system did not provide the intended ramps precisely, probably due to incorrect configuration of the acceleration parameters: the ramps to quench

illustrate roll off at high current, shown in Fig. 2. The tabulated ramp rates reflect the actual ramp rates measured in the quench data, but the dependence on ramp rate is weak.

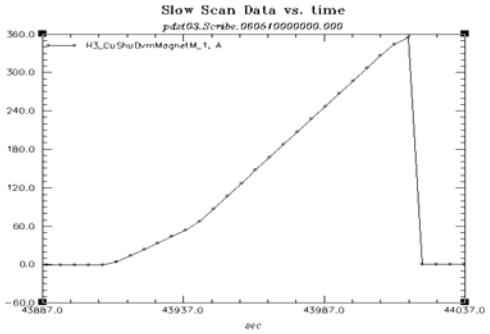

Fig. 2: Typical UNIX "Current (A) vs Time (s)" curve during a PDST03 ramp to quench.

Heater-Induced Quench Tests

Four quench heaters were located above the outer layer of the coil winding. The heater type was HK5591R12.9L12B, with individual resistance of 12.9 Ohm. The heater connection circuit was similar to that of PDST01-0, with a total resistance of ~13 Ω. A 4.9 Ω resister was added in parallel to the magnet heater circuit, so the HFU load resistance was 3.56 Ω. This resulted in an HFU pulse time constant of 8.5 ms, consistent with the measured time constant of ~ 8.4 ms. The measured dependence of quench delay on HFU Voltage and solenoid current is summarized Table 2 and plotted in Fig. 3.

Table 2: Delay of PDST03-0 quench onset (ms) vs HFU voltage and solenoid current.

U_{HFU} (V)	I = 200 A	I = 250 A	I = 300 A	I = 350 A
50	No Quench	No Quench	18	13
75	13	11	9	8
100	10	9	7	6
150	8	7	6	5.5

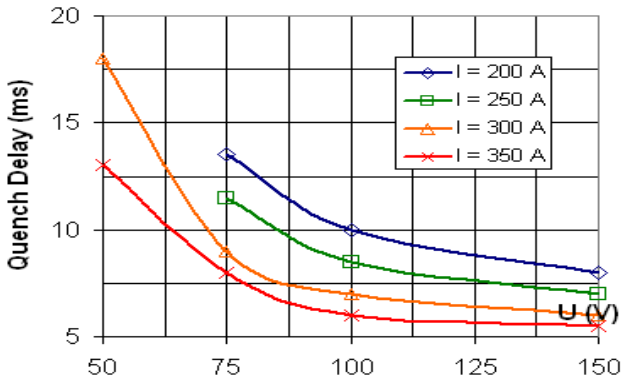

Fig. 3: Delay (ms) from heater firing to quench detection, as a function of V_{HFU} and Icoil

Solenoid Survival Test

Two unprotected quench events were initiated, in which all of the stored energy was deposited in the coil. Availability of voltage taps allowed quench propagation in the coil

to be measured. Graphs in Fig. 4 show voltage tap signals; the behavior of the curves in the graph can be interpreted in the following way:

1) While the coil is superconducting, I = const and R = 0, the total voltage is zero. If part of a layer surrounded by two voltage taps becomes normal, a positive (resistive) voltage is generated (e.g., see signals for T0/T2 and T2/T4 segments). Initially no inductive voltage is generated in this layer because of zero current derivative at t = 0.
2) As soon as the current starts decaying, negative (inductive) voltage adds to the positive resistive voltage making picture more complicated. There is a competition between the resistive and the inductive voltages in time and across the layers, as was shown in [5], depending on the current level and its decay rate.
3) When the current drops, the negative inductive voltage develops even across the layers that did not turn normal yet. For these layers, we see negative voltage first (T4/T6, T6/T10, T10/T14, and T14/T20), and later, when quench front comes to these layers, this voltage is compensated by positive resistive voltage rise.
4) As the current drops further, at different moments inductive or resistive voltage prevails resulting in several "oscillations" in the current shape.
5) With the current approaching "zero", both the resistive and the inductive components go to zero. At 300 ms, we see that the power source protection circuit is activated (it was set this way) and effectively dumps the remaining current into the dump resistor.

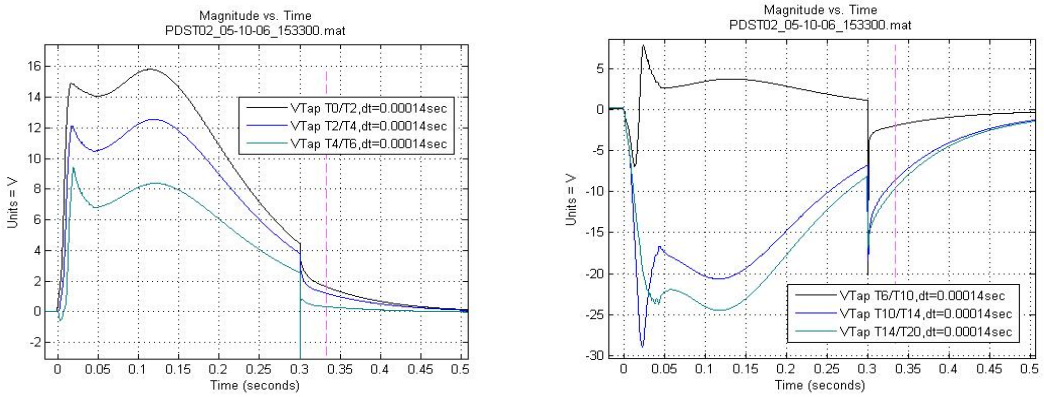

Fig. 4: Voltage tap signals in the unprotected quench event at 354.85 A

With this explanation of the signals, we can use the graphs to find when the resistive voltage starts developing in each section of the solenoid. Table 3 summarizes the measured quench delay for different layers of the PDST03 coil.

Table 3: Summary of quench development within PDST03-0 coil layers.

Layer #	2	4	6	10	14
Quench delay (ms)	2.5	5.0	14.0	23	40

Comparing this table with the results of quench propagation obtained in [4] for the current near quench (middle of the coil at ~ 12 ms and the whole coil at ~ 40 ms), we conclude that our understanding of what happens during a quench, which was based on the analysis performed in [4] and [5], is quite adequate.

Stress in the Solenoid

Fits to "resistance" versus "square of the current" were made to data from the two active gauges in the test solenoid, and Table 5 summarizes the results:

Table 5: Strain gauge resistance change with current

Fits of R vs I^2	Gage A	Gage B
$dR/dI^2 \cdot 10^6$ (Ω/A^2)	0.92 +/-0.01	0.89 +/-0.01

These slopes are slightly lower than those found for PDST01 and PDST02, but are certainly close (and the dependence is linear with squared current) as expected.

Magnetic Field Measurements

Magnetic measurements on PDST03 focused on magnetization properties of the conductor. Warm measurements prior to the cold test cycle were performed using the Kepko bipolar power supply to excite the coil with alternately positive, zero, negative, zero currents. The Hall probe was located at the solenoid center. A small residual magnetization at the level of 0.1 Gauss was noticed, presumably due to the presence of magnetic materials in the vicinity of the probe. This level at room temperature was deemed sufficiently small background for measuring the solenoid magnetization properties.

"Warm" and "cold" Z-scans were performed to locate the solenoid center, and to check the transfer functions; these are shown in Fig. 5 below. The warm data were taken before and after the cold test at 1 A with both polarities, while the cold data were taken at 100 Amperes in the coil following quench studies. The cold z-scan shows a slightly lower transfer function, presumably due to magnetization effects (discussed later). In the "warm" state, the peak transfer function is 200.5 ± 0.5 G/A; the predicted value is197.3.

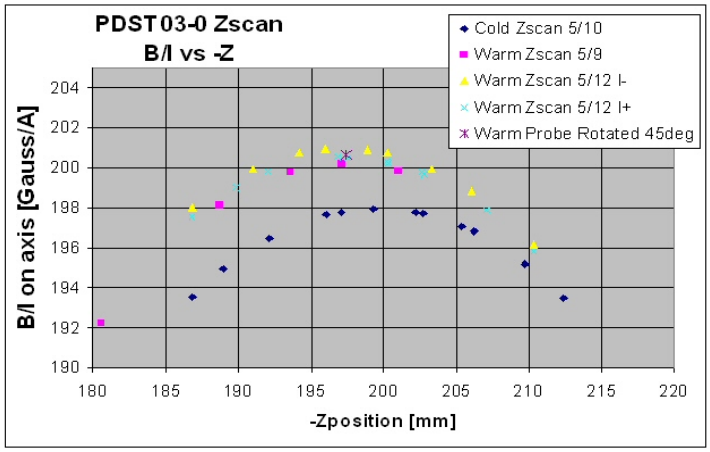

Fig. 5: PDST03-0 transfer function versus probe position from warm and cold z-scans.

Studying hysteresis preceded, and then followed quench studies (see Fig. 1); as the coil temperature profile following a quench is not known or predicted, the remnant magnetization state in the coil is also not predicted. For PDST03, power supply protection diodes were installed throughout the cold test, so this solenoid was excited with stair-step loops of only a single power supply polarity, and there is not a determination of the remnant field for bi-polar current cycles.

As was done for PDST02-0, the current plateaus were made 30 seconds duration, long enough for the current to stabilize at the same value on both the up and down ramp. The early stair step ramps showed surprisingly little hysteresis compared to similar loops for PDST02, and given our preliminary expectations. Therefore, following the quench studies, the same series of loops executed on PDST02 were again executed on PDST03 for a direct comparison of the width versus step size and maximum loop current. The widths of the hysteresis loop are shown as a function of the plateau current in Fig. 6 below, where we have determined the difference in magnetic field strength at a given plateau current between the down-going and the up-going legs of the hysteresis curve. This figure should be compared to Fig. 5 in [2]; it is clear that the behavior is very different, and the results were unexpected. Similar loops (5 A steps to 55 A, versus 5 A steps to 60 A) give very different hysteresis results, suggesting that coil excitation history is important. In the second ramp cycle, 10 A steps to 110 A, there appears to be an anomalously large width at 10A, but there is no indication of any problem with the measurements on either the up or down ramp.

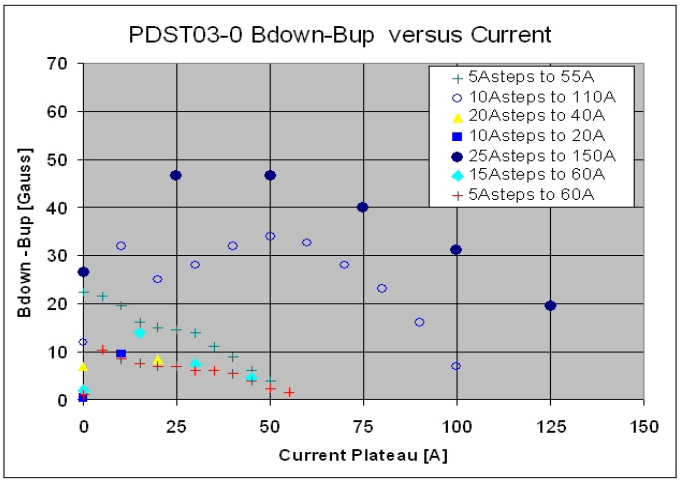

Fig. 6: Difference in solenoid central field versus stair-step current, [B↓–B↑], for unipolar hysteresis loops of varying step size and maximum current.

The magnetization data require additional analysis to understand this behavior. Because of this behavior, some care must be taken to ensure the solenoid fringe field does not exceed what is required by specifications.

Concluding Remarks

The Oxford strand coil PDST03 performed in a very similar way to the other two test solenoid magnets: characteristics of stress, quench and heater performance were all consistent with expectations; once again ramp rate dependence was fairly gentle, quench training was short and the magnet was self-protecting. Analysis of the voltage tap data shows nice agreement with the modeled quench development in the coil layers. Further analysis, modeling, and measurements of the strand properties are needed to understand the magnetization properties for solenoids made from either strand.

References

1. R. Carcagno, et al, Test Solenoids: Expected Performance and Test Results, Part 1: PDST01-0 and PDST01-1, TD-06-027, FNAL, July 2006.
2. R. Carcagno, et al, Test Solenoids: Expected Performance and Test Results, Part 2: PDST02-0, TD-06-028, FNAL, July 2006.
3. I. Terechkine, Proton Driver Front End. Warm Section Focusing Solenoid, TD-05-037, FNAL, August 2005
4. I. Terechkine, Focusing Solenoid Quench Protection Studies, pt. 1, TD-06-003, FNAL, January 2006
5. I. Terechkine, Focusing Solenoid Quench Protection Studies, pt. 2, TD-06-004, FNAL January 2006